Research Article | Vol. 37, No. 9 / August 2020 / Journal of the Optical Society of America A 1

Journal of the Optical Society of America A
OPTICS, IMAGE SCIENCE, AND VISION

Universal parameter to describe the reduction of refraction effects in the scattering of absorbing spheres

JUSTIN B. MAUGHAN* AND CHRISTOPHER M. SORENSEN

Department of Physics, Kansas State University, 116 Cardwell Hall, Manhattan, Kansas 66506-2601, USA
**Corresponding author: maughan@phys.ksu.edu*

Received 8 April 2020; revised 10 August 2020; accepted 11 August 2020; posted 11 August 2020 (Doc. ID 394401); published 0 MONTH 0000

The scattered intensity from large spheres with a real part of the refractive index of $n = 1.33, 1.5, 2.0$ is investigated as the radius R and an imaginary part of the refractive index κ are varied. It is shown that the product of κ and the size parameter kR, κkR, is a universal parameter describing the quenching of the refraction phenomenon of the scattered light: the refraction hump, the generalized rainbows, and the glory. The physical reason for this is that κkR is the inverse of the relative skin depth of light penetration into the sphere, which is demonstrated by calculations of the internal fields that darken universally as κkR increases.

https://doi.org/10.1364/JOSAA.394401

1. INTRODUCTION

One of the most well-known scattering phenomena, even to laypersons, is the rainbow. When incident white light interacts with roughly spherical water droplets there is a sharp increase in the amount of light that is scattered back at in the region of ∼135°. The exact angle of this increase is dependent upon the wavelength of the light, and thus for white light there is a separation of colors and hence the appearance of the rainbow. The rainbow is only one of the refraction effects found in the scattering from spherical particles. As some may have seen before, there are actually two rainbows, the secondary and the primary [1]. The rainbow is generally associated with water. However, spheres of indexes different from that of water have similar sharp increases in the amount of light scattered at specific angles depending on the refractive index; we will refer to these as "generalized rainbows."

Another refraction effect is the refraction hump when the scattering angle is in the range $\lambda/2R < \theta < 90° \sim 120°$ depending on the real part of the refractive index, where R is the sphere radius and λ is the wavelength of light [2,3]. There is also the glory; in water droplet clouds this is seen as colorful rings around the shadow of the observer when the shadow is cast upon a cloud [1]. The glory and hump, as with the rainbow, are not limited to water. The effects as seen in water are simply the most readily observable in daily life. Phillip Laven has done an immense amount of work studying refraction phenomena such as rainbows and glories. The interested reader is encouraged to explore his work; Refs. [4,5] are but two.

In this paper it will be shown that the product of the size parameter $kR = 2\pi R/\lambda$, and the imaginary part of the refractive index κ, κkR, provides a quasi-universal description of the reduction in the refractive effects due to absorption. The role the κkR parameter plays in describing the Rayleigh, geometric, and reflection regimes of the total absorption cross-section have already been presented in Ref. [6]. Our calculations here will be restricted to un-polarized incident light at a wavelength 532 nm, relatively large spheres, and the refractive indexes of $n = 1.33, 1.5, 2.0$ for the real part of the refractive index.

2. THEORY

Consider a plane mono-chromatic electromagnetic wave incident upon a homogenous sphere of radius R and a complex relative refractive index $m = n + i\kappa$, with n being the real part and κ the imaginary part. If the imaginary part of the refractive index is not equal to zero, then the wave will be attenuated as it travels in the sphere. The distance that the wave has traveled into the sphere when its amplitude has been attenuated to a factor of $1/e$ is known as the skin depth and is given by Ref. [7]

$$\delta = \frac{\lambda}{2\pi\kappa}. \tag{1}$$

The skin depth relative to the size of the sphere can then be expressed as follows:

$$\frac{\delta}{R} = \frac{\lambda}{2\pi\kappa R} = \frac{1}{\kappa kR}. \tag{2}$$

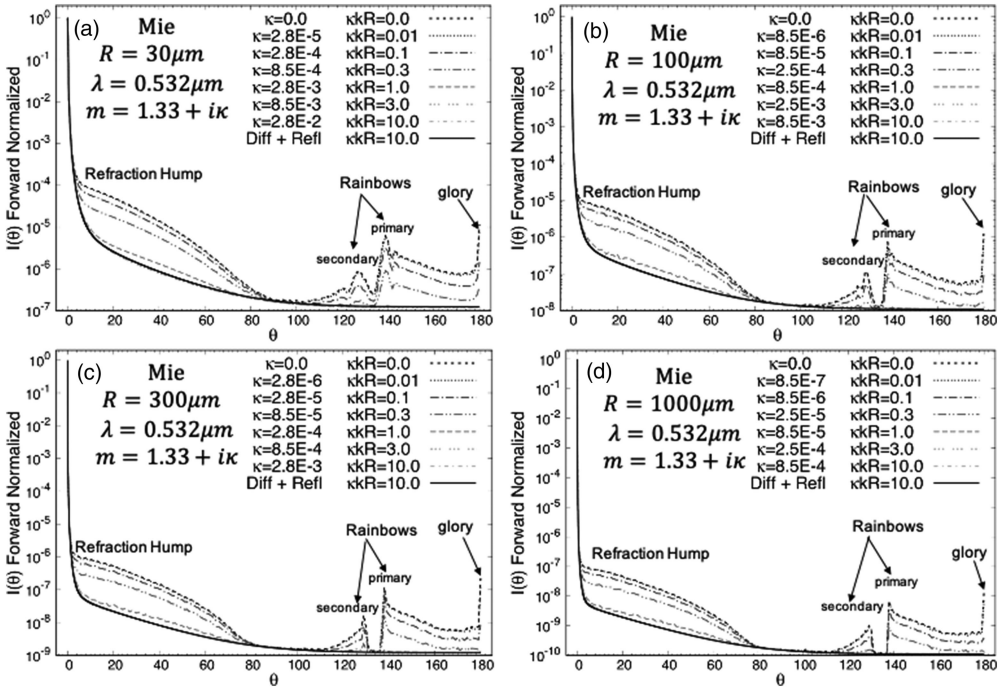

Fig. 1. Forward normalized scattered intensity versus the scattering angle θ (a). The Mie scattering for a sphere with a radius of 30 μm and an index of $m = 1.33 + i\kappa$. κ is varied so that $\kappa kR = 0$, 0.01, 0.03, 0.1, 0.3, 1, 3, 10. (b), (c), and (d) are the same as (a) but with radii of 100 μm, 300 μm, 1000 μm, respectively.

From Eq. (2) it can be seen that when the parameter $\kappa kR \ll 1$, the skin depth will be much larger than the sphere itself, and the effects of the absorption on the scattering will be minimal [8]. As κkR approaches unity, the skin depth becomes comparable to the size of the sphere and the refraction effects on the scattering start to become diminished. Ultimately, when $\kappa kR \geq 1$ the skin depth is at or less than R, and only an end "cap" on the side of the sphere that the wave is incident upon is illuminated. We expect that when $\kappa kR \geq 1$, most if not all of the refraction effects of the scattering should be gone and only the diffraction and reflection components of the scattering will be left [8]. The implication of Eq. (2) is that it is the combination κkR that controls the refraction effects of the scattering instead of either κ or the size parameter kR independently. In what follows we demonstrate that this is true and display the effects.

3. RESULTS

In Fig. 1 the forward normalized intensity of light scattered by spheres with a real part of refractive index $n = 1.33$ are plotted vs the scattering angle θ for radii of 30 μm, 100 μm, 300 μm, 1000 μm. The scattered intensity has been calculated using a Mie scattering code developed by our group, and has been tested against Phillip Laven's MiePlot [1]. A zero-order lognormal size distribution with a geometric width of $\sigma = 1.2$ has been used for the calculation of the scattering to wash out the ripple structure [9]. The real part of the refractive index is that of water with real part $n = 1.33$. The imaginary part of the refractive index is varied for each radius such that the κkR parameter ranges geometrically from 0 to 10.

The three main refraction effects can be seen in Fig. 1. First, for $\lambda/2R < \theta < 90°$ there is a feature that we call the refraction hump, which is followed by spikes in scattering at around 130° and 137.5°; these are the secondary and primary rainbow peaks, respectively. Between the secondary and primary rainbows is a dark region known as "Alexander's band" [1]. Finally, in the back direction as θ approaches 180° there is an increase in the refraction effect known as the "glory" [1].

The black curves in Fig. 1 are calculated based on [10], which lays out an asymptotic solution for large, highly absorbing particles. The asymptotic solution is reached essentially by disregarding any refraction into or out of the particle and thus

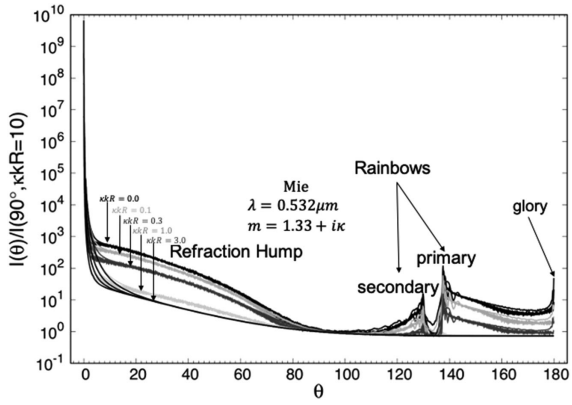

Fig. 2. Mie scattered intensity for spheres with radii of 30 μm, 100 μm, 300 μm, 1000 μm and an index of $m = 1.33 + i\kappa$. κ is varied so that $\kappa kR = 0$, 0.1, 0.3, 1, 3 all are normalized by the scattered intensity of a sphere of the same size and with $\kappa kR = 10$, at $\theta = 90°$, with the entire scattering angle range shown.

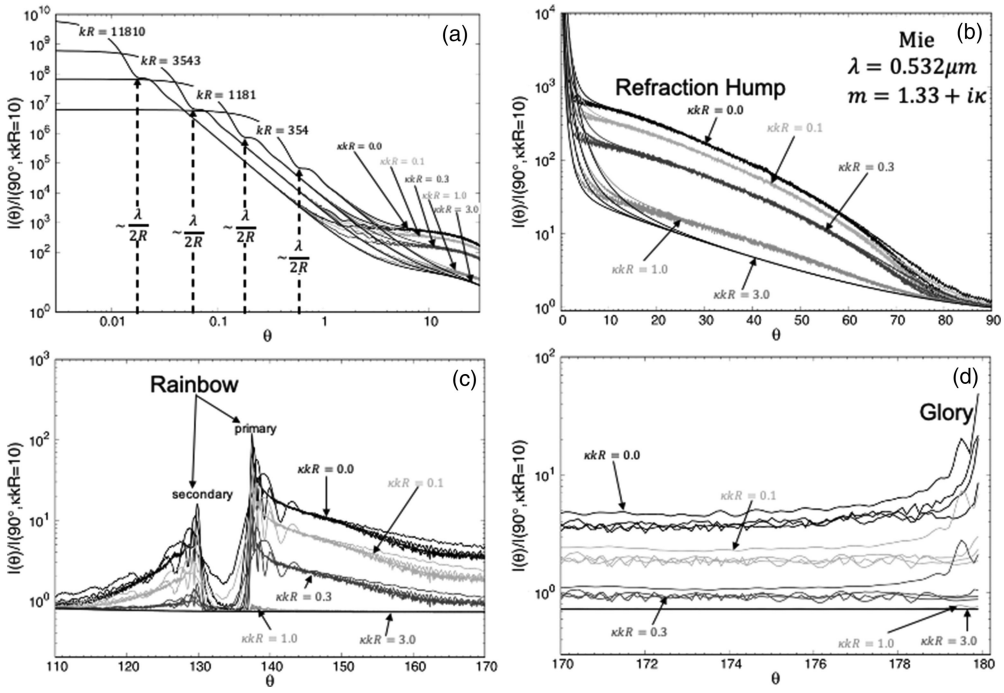

Fig. 3. Mie scattered intensity for spheres with radii of 30 μm, 100 μm, 300 μm, 1000 μm and an index of $m = 1.33 + i\kappa$. κ is varied so that $\kappa kR = 0$, 0.1, 0.3, 1, 3, all are normalized by the scattered intensity of a sphere of the same size and with $\kappa kR = 10$ at $\theta = 90°$, in four regions: (a) the forward scattering, which is dependent on kR; (b) the refraction hump; (c) the rainbows; and (d) the glory.

only leaves the sum of diffraction and reflection. Figure 1 shows that when $\kappa kR \leq 0.01$ the refraction effects are only slightly diminished. When $\kappa kR = 0.1$ there begins to be significant decreases in the refraction hump, rainbows, and the glory. The decreases in the refraction effects continue as κkR passes through 0.3. Once $\kappa kR = 1$, the scattering curves approach the sum of the diffraction and the reflection components of scattering and almost all the refraction effects are gone. With $\kappa kR \geq 3$, the scattering is equal to that of the sum of only the diffraction and reflection components. In Fig. 1 all four of the radii considered show a similar reduction in the refraction effects with the κkR parameter, despite having different kR and κ terms. It is important to take a moment to stress that κkR does not describe the refraction effects themselves but the reduction in them. We conclude that κkR is a universal parameter.

To further demonstrate the universality of κkR the scattering intensities from spheres with the same radii considered in Fig. 1 have been plotted together in Figs. 2 and 3. The full range of angles is shown in Fig. 2 and smaller ranges showing the individual refraction effects are shown in Fig. 3. As with Fig. 1, the imaginary part of the refractive index has been chosen such that there is a $\kappa kR = 0$, 0.1, 0.3, 1, 3 for each radius. The scattered intensity is normalized by the scattered intensity at $\theta = 90°$ from a sphere of the same radius, and with a kappa term such that $\kappa kR = 10$ in Figs. 2 and 3. This has been done for two reasons: (1) Fig. 1 shows that when $\kappa kR = 10$, essentially all the refraction effects have been removed, thus providing a common point of reference, and (2) forward normalization would not work because it depends on the size parameter kR, so using a forward normalization when comparing spheres of different size parameters would cause a separation in the curves [2,7].

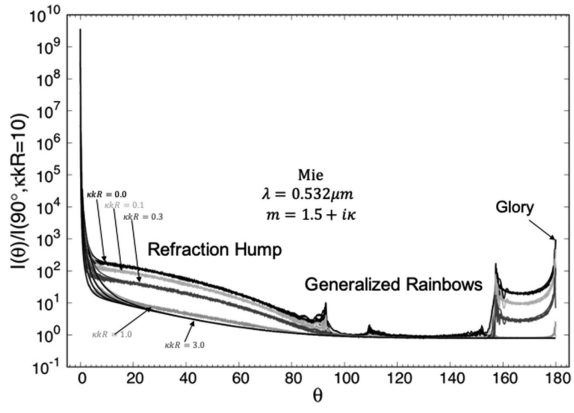

Fig. 4. Mie scattered intensity for spheres with radii of 30 μm, 100 μm, 300 μm, 1000 μm and an index of $m = 1.5 + i\kappa$. κ is varied so that $\kappa kR = 0$, 0.1, 0.3, 1, 3, all are normalized by the scattered intensity of a sphere of the same size and with $\kappa kR = 10$, at $\theta = 90°$, with the entire scattering angle range shown.

The dependence on kR can been seen in Fig. 3(a) in which the scattering up to $\theta = 30°$ is plotted on a log-log plot to emphasize the forward scattering. In Fig. 3(a) it is clear that curves with the same kR group scatter together in the forward directions. For large kR the scattering in the forward directions is described by the diffraction from a circular obstacle (or aperture) and has a first minimum at $\sim\lambda/2R$ [2,7]. After the first minimum in Fig. 3(a) the curves of similar kR separate and transition into the refraction hump, where the curves begin to group according to κkR instead of just kR.

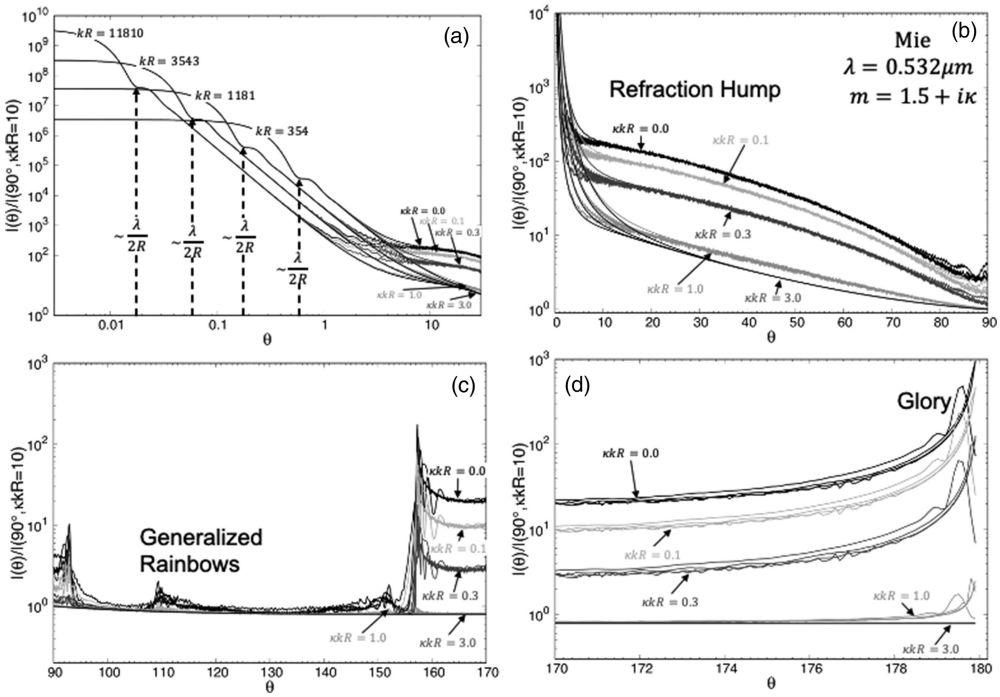

Fig. 5. Mie scattered intensity for spheres with radii of 30 μm, 100 μm, 300 μm, 1000 μm and an index of $m = 1.5 + i\kappa$. κ is varied so that $\kappa kR = 0, 0.1, 0.3, 1, 3$ all are normalized by the scattered intensity of a sphere of the same size and with $\kappa kR = 10$, at $\theta = 90°$, in four regions: (a) the forward scattering, which is dependent on kR; (b) the refraction hump; (c) the rainbows; and (d) the glory.

Figure 3(b) shows the refraction hump when $\lambda/2R < \theta < 90°$. The reduction in the refraction hump from its largest value when $\kappa kR = 0$ to no hump when $\kappa kR = 3$ is described well with κkR, despite the individual spheres with the same κkR having different size parameters kR and κ terms. Similarly, in Fig. 3(c) the refraction rainbows' effects are systematically reduced by κkR. In Fig. 3(d) for the glory regime when $170° \le \theta \le 178.5°$ there is similar systematic behavior in the reduction of the refraction effect, as seen in Figs. 3(b) and 3(c). However, the reduction appears to be more sensitive to κkR in the back directions. By the time $\kappa kR = 1$, all refraction effects appear to have been reduced and there is no difference between $\kappa kR = 1$ and $\kappa kR = 3$, whereas in Fig. 3(b) there is a distinction between $\kappa kR = 1$ and $\kappa kR = 3$. As θ approaches 180° the groups of similar κkR start to separate somewhat as the back directions are extremely sensitive to both the real and imaginary refractive indexes as well as size [11]. However, the reduction in the effects with increasing κkR is still similar.

Figures 4–7 are similar to Figs. 2 and 3 except with a real part of the refractive index in Figs. 4 and 5 of $n = 1.5$, while Figs. 6 and 7 are produced with a real part of $n = 2.0$. Figs. 5(b) and 7(b) show refraction humps, with the reduction from $\kappa kR = 0$ to no hump when $\kappa kR = 3$, again described well by κkR, despite the spheres with the same κkR having different size parameters kR and κ terms. Figure 5(c) shows the generalized rainbow for $n = 1.5$, which shows a similar systematic reduction with κkR as was seen with $n = 1.33$. Figure 7(c) shows only part of the generalized rainbow for $n = 2.0$; this is due to the fact that the primary rainbow has been pushed to a scattering angle of 180° and combines with the glory. Nevertheless, Fig. 7(c) shows a similar systematic reduction with κkR as was seen with

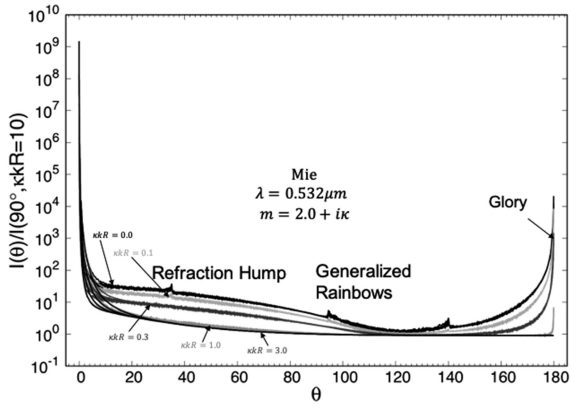

Fig. 6. Mie scattered intensity for spheres with radii of 30 μm, 100 μm, 300 μm, 1000 μm and an index of $m = 2.0 + i\kappa$. κ is varied so that $\kappa kR = 0, 0.1, 0.3, 1, 3$ all are normalized by the scattered intensity of a sphere of the same size and with $\kappa kR = 10$, at $\theta = 90°$, with the entire scattering angle range shown.

$n = 1.33$ and $n = 1.5$. Figures 5(d) and 7(d) show the glories as θ approaches 180° and once again there is a similar systematic reduction of the glories described by κkR, further demonstrating the universality of the κkR parameter. However, in the last two degrees of the scattering shown in Figs. 5(b) and 7(b), there is a separation between curves for $\kappa kR = 1$ and $\kappa kR = 3$, unlike in Fig. 3(b).

The increase as θ approaches 180° can be understood by looking at the $p = 2$ term of the Debye series [1]. The $p = 2$ is associated with rays that have a single internal reflection within

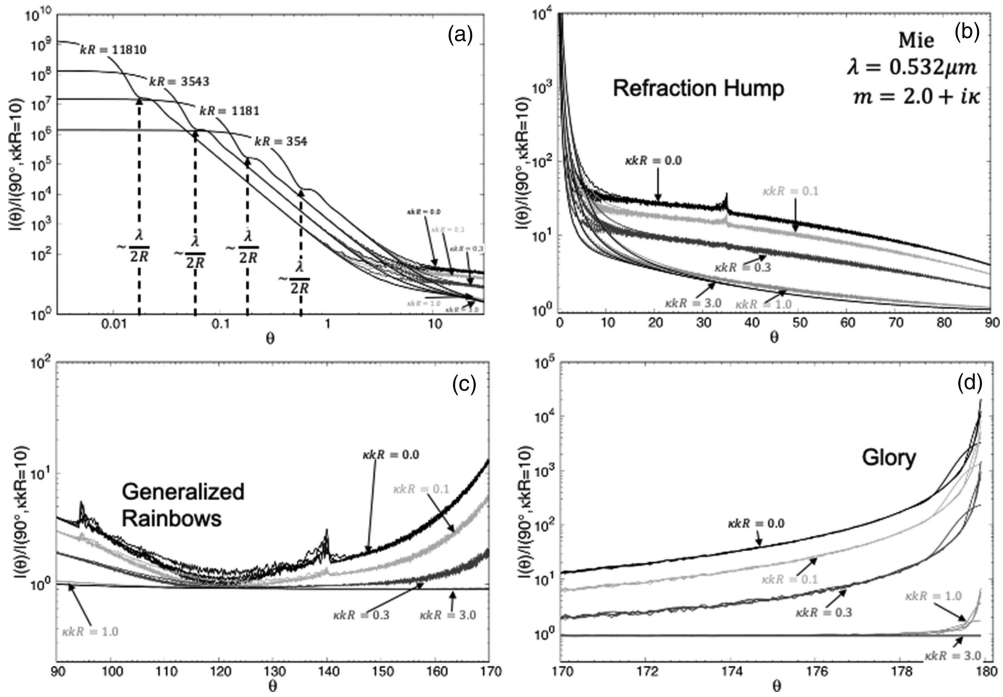

Fig. 7. Mie scattered intensity for spheres with radii of 30 μm, 100 μm, 300 μm, 1000 μm and an index of $m = 2.0 + i\kappa$. κ is varied so that $\kappa kR = 0$, 0.1, 0.3, 1, 3 all are normalized by the scattered intensity of a sphere of the same size and with $\kappa kR = 10$, at $\theta = 90°$, in four regions: (a) the forward scattering, which is dependent on kR; (b) the refraction hump; (c) the rainbows; and (d) the glory.

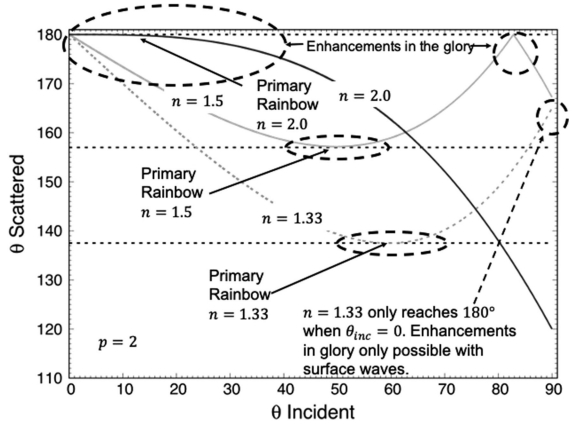

Fig. 8. The scattering angles vs the angle of incidence for the $p = 2$ rays, which have one internal reflection. The curves shown are for a real part of the refractive index $n = 1.33$, $n = 1.5$, $n = 2.0$; the horizontal dashed lines indicate the primary rainbow.

the sphere. The scattering angle θ can be related to the angle of incidence of a ray θ_i by Ref. [4]

$$\theta = (p-1)180° + 2\theta_i - 2p\,\mathrm{Sin}^{-1}(\mathrm{Sin}(\theta_i)/n). \quad \textbf{(3)}$$

As shown in Fig. 8 for $n = 1.33$, when the index of refraction is less than $n < \sqrt{2}$ the only $p = 2$ rays that scatter at 180° are those with an incident angle of 0°; these are rays that pass directly down the center of the sphere and reflect once off the inner front face of the sphere and back out at 180°. At iincident angles close to 0°, the $p = 2$ rays will travel similar path lengths and constructively interfere and add to the glory scattering angles close to 180° at any index of refraction [4]. For the refractive index of water $n = 1.33$, the glory is considered to be the sum of the effects of the $p = 2$ rays when the incident angle is small and the interference of $p = 2$ rays produce surface waves in such a fashion that the rays travel the same path length and also interfere constructively [4]. Figure 8 also demostrates that the $p = 2$ rays play a dominant role in the formation of the primary rainbows. When the slope of a curve in Fig. 8 is zero there is a range of incident angles that all scatter in the same direction. The primary rainbow angle of 137.5° has been marked in Fig. 8, and it can be seen that it coincides with the zero slope for $n = 1.33$.

When $n \geq \sqrt{2}$ the $p = 2$ rays also have at least one incident angle other than at 0° that scatter at 180°. These rays will constructively interfere with the rays that have an equal but opposite incident angle entering on the other side of the sphere. It is the direct interference of these $p = 2$ rays that leads to the glories seen in Figs. 5(b) and 7(b). There is a small distinction in the underlying cause of the glory in Fig. 3(b) when compared to that in Figs. 5(b) and 7(b) due to differing refraction effects. However, κkR still does well at describing the reduction in those effects as expected. Also in Fig. 8 it can be seen that the primary rainbow when $n = 1.5$ is also predominantly a $p = 2$ ray effect. When $n = 2.0$, the primary rainbow in Figs. 6 and 7(b) is difficult to identify. This is because the primary rainbow and the glory have combined and both effects are scattering at the same angles. Evidence of this is shown in Fig. 8, where there is a slope of zero for the first the 20° and the first 50° of incident angles are all scattering between 170° and 180°.

To investigate further the universal behavior with κkR, Figs. 9–13 show the magnitude of the internal fields and the

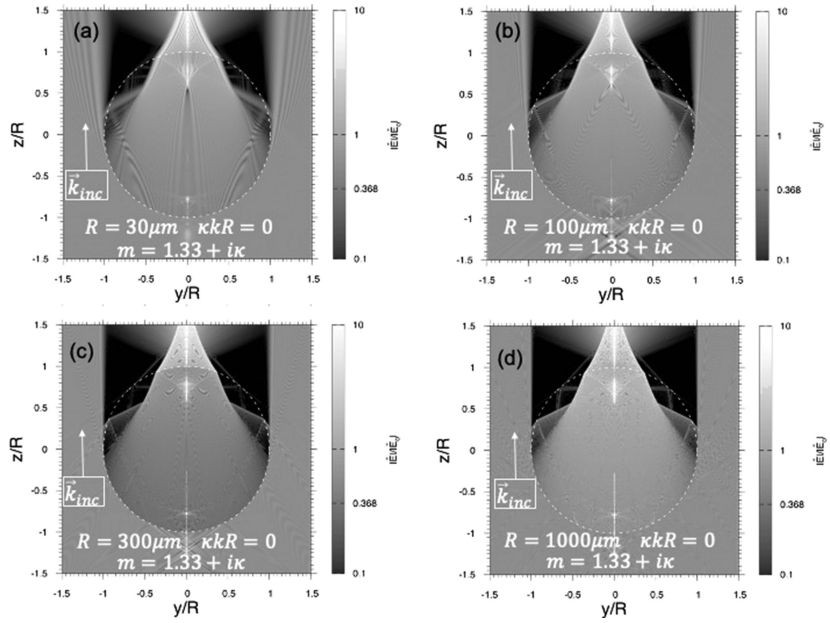

Fig. 9. (a) Relative internal and near field amplitudes for a slice of the sphere at $x = 0$ and with a radius of 30 μm and an index of $m = 1.33 + i0$ with a $\kappa kR = 0$. (b), (c), and (d) are the same as (a) but with radii of 100 μm, 300 μm, 1000 μm, respectively.

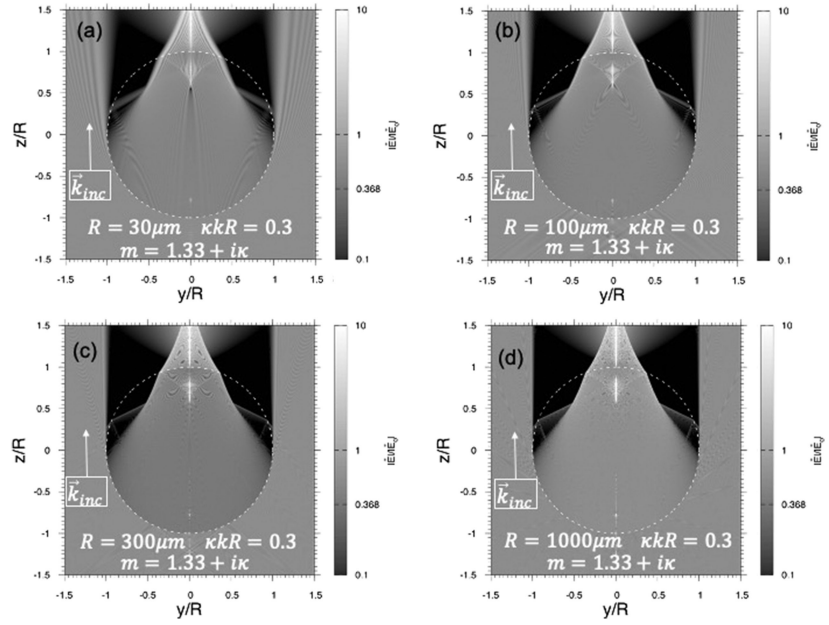

Fig. 10. (a) Relative internal and near field amplitudes for a slice of the sphere at $x = 0$ and with a radius of 30 μm and an index of $m = 1.33 + i0$ with a $\kappa kR = 1/3$. (b), (c), and (d) are the same as (a) but with radii of 100 μm, 300 μm, 1000 μm, respectively.

fields close to the surface of the spheres, relative to the magnitude of the incident field for the four radii being considered. In these plots a two-dimensional slice in the scattering ($x = 0$) plane is shown, and the y and z axis have been scaled by the radius of the sphere R. In each of the plots a white dash unit circle that represents the radius of the sphere is shown. The incident field direction of propagation is $\vec{k}_{\text{inc}}$ in the positive z direction and the light is unpolarized. The colors represent the relative magnitude of the fields, with orange and yellow being larger than the incident field. Reds are approximately equal to the incident field, while violets and purples are below it; the $1/e = 0.368$ value is in this range. Finally, blacks are at or below $1/10$ of the incident field.

Figure 9 shows the non-absorbing case when $\kappa = 0$ and thus $\kappa kR = 0$. Figure 9 shows that the relative fields are very similar despite the spheres being different sizes. Some of the similarities include bright areas within and in the near field in the forward direction along the y/R axis. On either side of the bright areas in the $\pm y/R$ directions both within and outside the spheres there are some darker regions in all four spheres. Within the rest of the

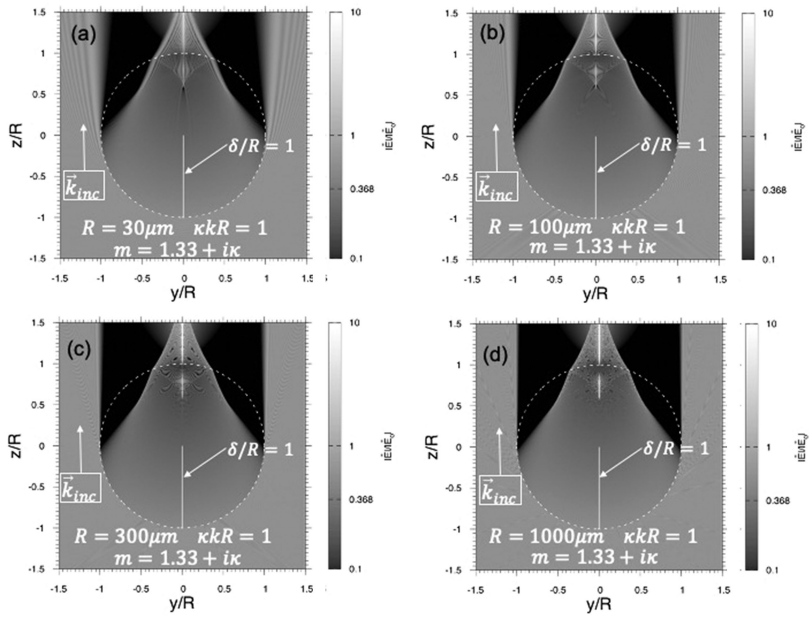

Fig. 11. (a) Relative internal and near field amplitudes for a slice of the sphere at $x = 0$ and with a radius of 30 μm and an index of $m = 1.33 + i\kappa$ with κ set so that $\kappa kR = 1$. The white line in the center marks the relative skin depth. (b), (c), and (d) are the same as (a) but with radii of 100 μm, 300 μm, 1000 μm, respectively.

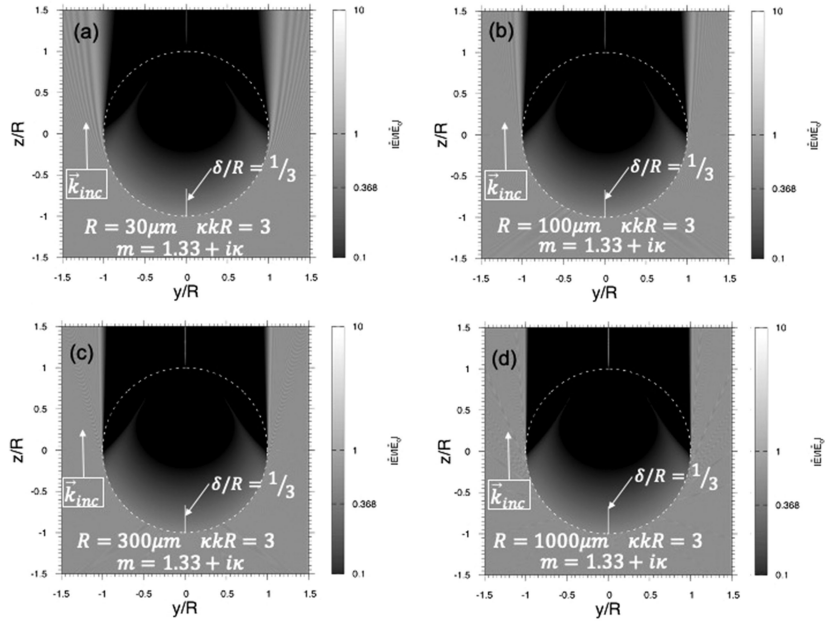

Fig. 12. (a) Relative internal and near field amplitudes for a slice of the sphere at $x = 0$ and with a radius of 30 μm and an index of $m = 1.33 + i\kappa$ with κ set so that $\kappa kR = 3$. The white line in the center marks the relative skin depth. (b), (c), and (d) are the same as (a) but with radii of 100 μm, 300 μm, 1000 μm, respectively.

sphere the internal field is relatively close to or below that of the incident field. All these features are consistent with a ray optics description of the internal wave in these large spheres.

In Fig. 10, despite being different sizes and having different κ values, all of the spheres have the same κkR parameter and thus the same relative skin depth of $\delta/R = 3$. While not identical it can be seen that the relative field magnitudes of all four of the spheres in Fig. 10 are similar and have changed similarly when compared to those in Fig. 9. The bright areas have dimmed, and the dark regions have expanded slightly. The relative skin depths are still larger than the diameter of the spheres, and so the changes thus far are minimal.

In Fig. 11 the spheres have the same κkR parameter and thus the same relative skin depth of unity, but now the relative skin depth is less than the diameter of the spheres. Again, they are not identical, but it can be seen that the relative field magnitudes of

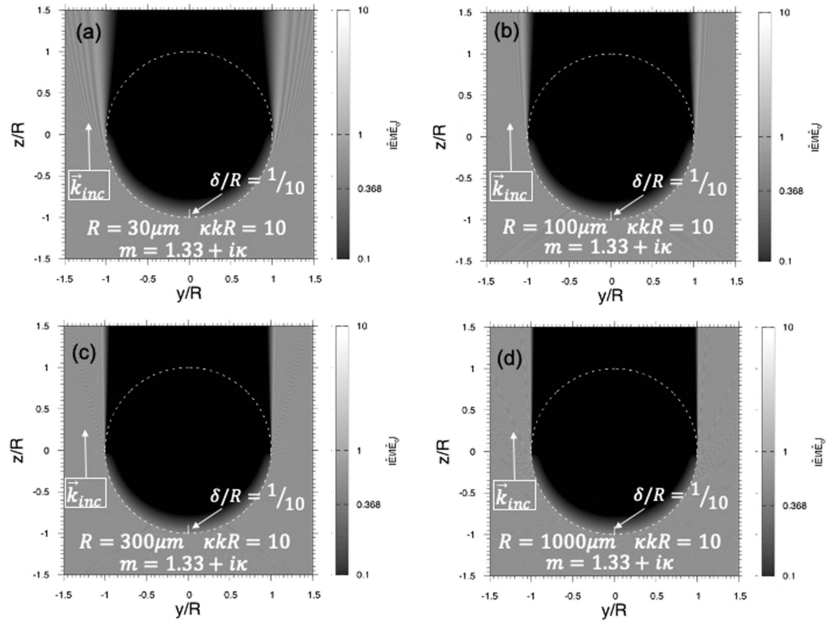

Fig. 13. (a) Relative internal and near field amplitudes for a slice of the sphere at $x = 0$ and with a radius of 30 μm and an index of $m = 1.33 + i\kappa$ with κ set so that $\kappa kR = 10$. The white line in the center marks the relative skin depth. (b), (c), and (d) are the same as (a) but with radii of 100 μm, 300 μm, 1000 μm, respectively.

all four of the spheres in Fig. 11 are similar and have changed similarly when compared to those in Fig. 10. The bright areas have significantly dimmed and the dark regions with relative fields at or less than 0.1 of the incident field have expanded. The majority of the internal fields that were at or just below the incident field have also dimmed.

Similar to Fig. 11, all four of the plots in Fig. 12 have the same $\kappa kR = 3$ and the same relative skin depth $\delta/R = 1/\kappa kR = 1/3$. It is clear in Fig. 12 that the relative field magnitudes inside the spheres are almost identical despite having different kR and κ terms. In Fig. 12 the bright areas are gone, the dark regions have merged, and all of the fields within the sphere are smaller than those in the incident field. Also, in Fig. 12 it can be seen that the relative skin depth δ/R describes well the $1/e = 0.368$ point. Figure 13 is similar to Figs. 11 and 12, but with $\kappa kR = 10$, now almost the entire sphere is dark and all that remains is an illuminated "cap" on the side of the sphere that the wave is incident upon. Going through Figs. 9–13, the similarities in the internal fields of the spheres with the same κkR support the conclusion that κkR is a universal parameter with universal consequences for scattering, as shown in Figs. 1–7.

4. CONCLUSIONS

It has been shown that the imaginary part of the refractive index is responsible for a reduction in the refraction effects of scattering by large spheres. However, it is not the magnitude of κ, but rather the magnitude of the parameter κkR that quantitatively describes the reduction of the refraction effects. The refraction effects are the refraction hump, the generalized rainbows, and the glory. Said differently, it is not whether κ is small or large that determines low- or high- absorption effects of the scattering. Instead, low-absorption effects occur when $\kappa kR < 0.1$ and high-absorption effects occur when $\kappa kR \geq 1$, regardless of the individual values of κ and kR. The physical explanation for this is that κkR is equal to the relative skin depth for penetration of the light into the sphere. This was demonstrated by the calculations of the internal fields of spheres. Thus, spheres with the same κkR parameter will have the same reduction in the internal fields and hence the same reduction of the refraction effects when compared to a sphere with $\kappa kR = 0$. Once $\kappa kR \sim 3$ has been reached, the refraction effects have been almost totally quenched and the scattering only consists of diffraction and reflection effects. We expect the κkR parameter provides some degree of universal control of refraction effects in the scattering by spheres of other sizes and real refractive indices as well as scattering by non-spherical particles.

Funding. National Science Foundation (AGM 1649783).

Disclosures. The authors declare no conflicts of interest.

REFERENCES

1. P. Laven, "Simulation of rainbows, coronas and glories using Mie theory and the Debye series," J. Quant. Spectrosc. Radiat. Transfer **89**, 257–269 (2004).
2. W. R. Heinson, A. Chakrabarti, and C. M. Sorensen, "Crossover from spherical particle Mie scattering to circular aperture diffraction," J. Opt. Soc. Am. A **31**, 2362–2364 (2014).
3. Y. W. Heinson, J. B. Maughan, J. Ding, A. Chakrabarti, P. Yang, and C. M. Sorensen, "Q-space analysis of light scattering by ice crystals," J. Quant. Spectrosc. Radiat. Transfer **185**, 86–94 (2016).
4. P. Laven, "How are glories formed?" Appl. Opt. **44**, 5675–5683 (2005).
5. P. Laven, "Effects of refractive index on glories," Appl. Opt. **47**, H133–H142 (2008).

6. C. M. Sorensen, J. B. Maughan, and H. Moosmueller, "Spherical particle absorption over a broad range of imaginary refractive index," J. Quant. Spectrosc. Radiat. Transfer **226**, 81–86 (2019).
7. E. Hecht, *Optics*, 2nd ed. (Addison-Wesley, 1987).
8. G. Wang, A. Chakrabarti, and C. M. Sorensen, "Effect of the imaginary part of the refractive index on light scattering by spheres," J. Opt. Soc. Am. A **32**, 1231–1235 (2015).
9. M. Kerker, *The Scattering of Light and Other Electromagnetic Radiation: Physical Chemistry: A Series of Monographs* (Academic, 2016).
10. P. Yang, B.-C. Gao, B. A. Baum, Y. X. Hu, W. J. Wiscombe, M. I. Mishchenko, D. M. Winker, and S. L. Nasiri, "Asymptotic solutions for optical properties of large particles with strong absorption," Appl. Opt. **40**, 1532–1547 (2001).
11. B. M. Heffernan, Y. W. Heinson, J. B. Maughan, A. Chakrabarti, and C. M. Sorensen, "Backscattering measurements of micron-sized spherical particles," Appl. Opt. **55**, 3214–3218 (2016).

Queries

1. AU: As per the style, Manuscript title should not begin with an article "A". So it has been deleted. Please check and confirm.

2. AU: It is unclear what Eq. 1 relates to.Please indicate whether Eq. 1 shows the skin depth (and what is given by Ref. 7). If so, consider changing the sentence leading into the equation as "is known as the skin depth, is given by Ref [7], and is as follows:"

3. AU: The funding information for this article has been generated using the information you provided to OSA at the time of article submission. Please check it carefully. If any information needs to be corrected or added, please provide the full name of the funding organization/institution as provided in the CrossRef Open Funder Registry (https://search.crossref.org/funding).